Scaling Up Electronic Structure Calculations on Quantum Computers: The Frozen Natural Orbital Based Method of Increments

Prakash Verma,[1] Lee Huntington,[1] Marc Coons,[2] Yukio Kawashima,[1] Takeshi Yamazaki,[1, a)] and Arman Zaribafiyan[1]

[1)] *1QB Information Technologies Inc. (1QBit)*

[2)] *Dow Inc.*

Quantum computing is a new computing paradigm that holds great promise for the efficient simulation of quantum mechanical systems. However, the hardware envelope provided by noisy, intermediate-scale quantum (NISQ) devices is still small compared to the size of molecules that are relevant to industry. In the present paper, the method of increments (MI) is introduced to help expedite the application of NISQ devices for quantum chemistry simulations. The MI approach expresses the electron correlation energy of a molecular system as a truncated many-body expansion in terms of orbitals, atoms, molecules, or fragments. Here, the electron correlation of the system is expanded in terms of occupied orbitals, and the MI approach is employed to systematically reduce the occupied orbital space. At the same time, the virtual orbital space is reduced based on the frozen natural orbitals (FNO), which are obtained using a one-particle density matrix from second-order, many-body perturbation theory. In this way, a method referred to as the MI-FNO approach is constructed for the systematic reduction of both the occupied space and the virtual space in quantum chemistry simulations. The subproblems resulting from the MI-FNO reduction can then be solved by any algorithm, including quantum algorithms such as the phase estimation algorithm and the variational quantum eigensolver, to predict the correlation energies of a molecular system. The accuracy and feasibility of the MI-FNO approach are investigated for the case of small molecules—i.e., BeH_2, CH_4, NH_3, H_2O, and HF—within a cc-pVDZ basis set. Then, the efficacy of the proposed framework is investigated for larger molecules used in realistic industrial applications using a qubit-count estimation on an industrially relevant, medium-sized catalyst molecule, the "constrained geometry" olefin polymerization catalyst. We show that, even by employing a modest truncation of the virtual space, the MI-FNO approach reduces the qubit requirement by almost a factor of one half. In doing so, our approach can facilitate hardware experiments based on smaller, yet more realistic, chemistry problems, assisting in the characterization of NISQ devices. Moreover, reducing the qubit requirement can help scale up the size of molecular systems that can be simulated in quantum chemistry applications, which can greatly enhance computational chemistry studies for large-scale industrial applications.

I. INTRODUCTION

The computational prediction of chemical processes requires an accurate description of the quantum nature of the molecules involved. However, the simulation of quantum mechanical systems on classical computers is a computationally demanding task, as the dimension of the Hilbert space of quantum systems increases exponentially with system size. Thus, on classical hardware, exact solutions of the molecular, electronic Schrödinger equation are only possible for small systems[1].

There has been increasing interest in quantum computation, a new computing paradigm initially conjectured as an efficient framework for simulating quantum mechanical systems[2,3]. In the decades since this conjecture was put forward, there has been tremendous theoretical progress towards proving the concept of using a quantum computer for quantum simulations[4], and early demonstrations of quantum algorithms were implemented[5] and tested for the study of molecular energies on a quantum computer[6–10]. There has also been accelerated progress in hardware development. For example, IBM[11], Google[12], Intel[13], Rigetti[14], and QCI[15] have all developed quantum computing platforms based on superconducting qubits, while IonQ[16] and Honeywell[17] have developed platforms based on ion traps. Googles achievement on a benchmarking milestone commonly referred to as "quantum supremacy"[18] is a demonstration of the transitioning of quantum computers away from being merely a theoretical concept. Despite this accelerated progress, existing quantum hardware remains error-prone and limited in computing capacity, hence the introduction of the term noisy, intermediate-scale quantum (NISQ) device[19]. Error correction and fault tolerance are the keys to scalable

---

[a)] Electronic mail: takeshi.yamazaki@1qbit.com

quantum computers. However, current devices are both too noisy and too limited in the number of qubits to be able to perform error correction. In parallel, while the resources required for simulating quantum systems on quantum hardware can scale better than on classical computers, they still require qubit counts, gate fidelities, and a level of coherence beyond the limitations of currently available NISQ devices.

Great effort has been made towards overcoming the limitations of NISQ devices, and to accelerate the application of quantum computing to quantum chemistry by introducing quantum–classical hybrid algorithms[20–23], low-depth circuit ansatzes for quantum simulation[24–31], and problem decomposition techniques (PD) from quantum chemistry[32–37]. Reducing the problem size of a molecular system is essential for the NISQ era. Such a reduction can provide us with more opportunities to characterize near-term devices, allowing us to conduct hardware experiments based on larger systems rather than the toy problems that are currently accessible.

The PD techniques of quantum chemistry are approximations used to study a molecule or a material by decomposing the electronic structure calculation problem of a given system into subproblems for more-efficient calculations, without a great sacrifice in accuracy. These approaches have a very long history, beginning with the early work of Sinanoğlu[38], Nesbet[39], and Ahlrichs and Kutzelnigg[40] on local correlation in the 1960s. Reviews on some PD techniques in quantum chemistry and references are readily available[41–44]. Of particular note are the recent development of local pair natural orbital based coupled-cluster (CC) approaches[45–51] that allow calculations to be performed on much larger systems than their parent canonical CC approaches.

The application of PD techniques in quantum chemistry simulations on quantum computers has been proposed in several studies. Such work includes the active space approach, including only the important occupied and virtual orbitals into the computational space[33,35]; the reduction of the virtual orbital space by removing higher eigenvalue canonical virtual orbitals[52]; and the systematic reduction of the virtual space based on the frozen natural orbital (FNO) method[52,53]. These approaches are useful for reducing problem size; however, to our knowledge, no approach has been proposed for the systematic reduction of both the occupied space and the virtual space. The systematic truncation of the occupied space also becomes essential, in particular, when larger molecular systems that have a considerable number of electrons are targeted.

An incremental full configuration interaction (iFCI) approach based on the method of increments has been recently proposed[54–56], which provides a polynomial scaling approximation to full configuration interaction (FCI). By decomposing the problem into n-body subproblems (or "increments"), it has been shown that accurate correlation energies can be recovered at low values of n in a highly parallelizable computation[54–56].

In the present study, we use the method of increments (MI) to reduce the occupied space of a molecular system, and the FNO method[57–61] to truncate virtual space. In this way, a novel framework, which we call the MI-FNO approach, is constructed for the systematic reduction of both the occupied and the virtual spaces in the context of quantum chemistry simulations on near-term quantum devices. As a first step, we validate the accuracy of the MI-FNO approach, and demonstrate its ability to reduce both the occupied and virtual spaces while maintaining a reasonable level of accuracy, by examining the small molecules BeH_2, CH_4, NH_3, H_2O, and HF using a moderate-sized cc-pVDZ basis set[62]. Then, as an early demonstration of the efficacy of our MI-FNO approach on larger molecules, we give a qubit count estimation for an industrially relevant, medium-sized catalyst molecule (the "constrained geometry" olefin polymerization catalyst) using the cc-pVDZ and cc-pVTZ basis sets[62].

This paper is organized as follows. In Sec. II, a review of the MI, FNO, and the variational quantum eigensolver (VQE) is provided as an example of the quantum solvers suitable for near-term quantum devices. In Sec. III, the computational details are described and a schematic illustration is provided of our MI-FNO approach for large-scale quantum chemistry simulations on quantum hardware. In Sec. IV, we present the resulting molecular energies obtained with the MI-FNO approach and discuss its applicability for use on near-term devices. Sec. V concludes the paper, providing a summary of results and possibilities for future work.

Similar to our previous work[36], the present study is an attempt to build an efficient framework for performing scalable quantum chemistry simulations on near-term devices based on PD techniques.

II. THEORY

Figure 1 shows a conceptual illustration of the MI-FNO framework. In this section, we provide a brief overview of each ingredient comprising the framework, namely, the method of increments (MI) to distribute the occupied orbitals among subproblems (or "increments" in the context of MI) and the use of FNOs to restrict the number of virtual orbitals within each subproblem. The VQE is presented as an example of the possible quantum solvers for near-term quantum devices. The framework is compatible with other quantum algorithms and, more generally, with both quantum and classical back ends for solving the subproblems.
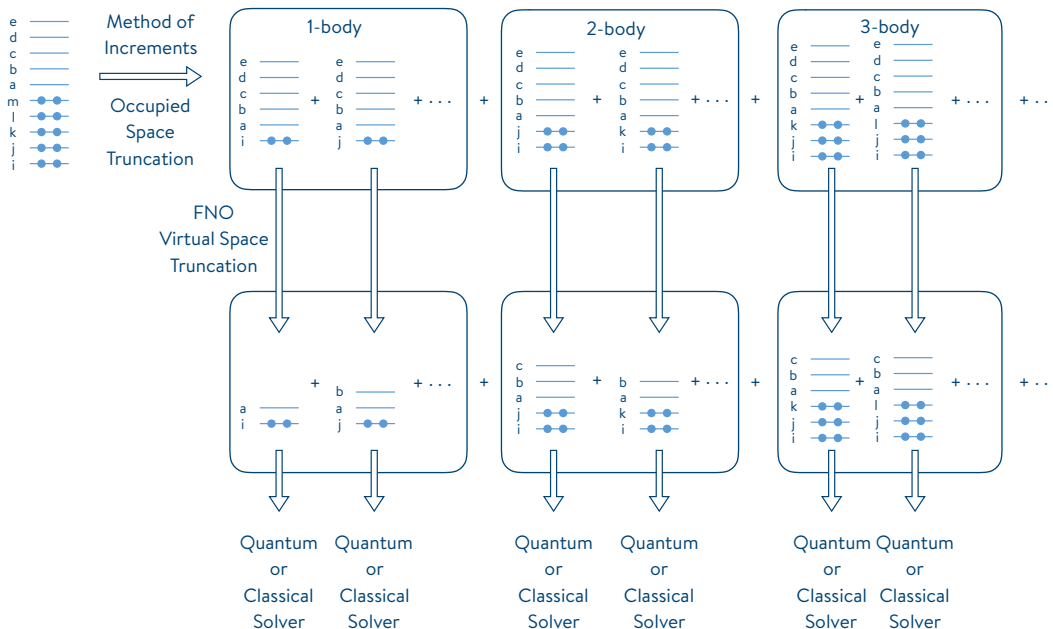
FIG. 1. Conceptual and schematic illustration of the MI-FNO framework for scaling up the size of molecules for quantum chemistry simulations on quantum hardware

A. Method of increments

The MI approach, first introduced in quantum chemistry by Nesbet[63–65], is based upon the n-body Bethe–Goldstone expansion[66] of the correlation energy of a molecule. The correlation energy (E_c), defined as the difference between the exact (E_{exact}) and the Hartree–Fock (mean-field) energy (E_{HF}), can be expanded as

$$
\begin{aligned}
E_c &= E_{\text{exact}} - E_{\text{HF}} \\
&= \sum_i \epsilon_{\text{i}} + \sum_{i>j} \epsilon_{ij} + \sum_{i>j>k} \epsilon_{ijk} + \sum_{i>j>k>l} \epsilon_{ijkl} \cdots ,
\end{aligned}
\tag{1}
$$

where ϵ_i, ϵ_{ij}, ϵ_{ijk}, and ϵ_{ijkl} are, respectively, the one-, two-, three-, and four-body increments (expansions) defined as

$$
\epsilon_i = E_c(i) \tag{2}
$$
$$
\epsilon_{ij} = E_c(ij) - \epsilon_i - \epsilon_j \tag{3}
$$
$$
\epsilon_{ijk} = E_c(ijk) - \epsilon_{ij} - \epsilon_{ik} - \epsilon_{jk} - \epsilon_i - \epsilon_j - \epsilon_k \tag{4}
$$
$$
\epsilon_{ijkl} = E_c(ijkl) - \epsilon_{ijk} - \epsilon_{ijl} - \epsilon_{jkl} - \cdots \tag{5}
$$
$$
\vdots
$$

where $E_c(i)$ denotes the correlation energy of the increment i.

Depending on the type of increments we use, the indices (i, j, k, ...) appearing in the expansion of Eq. 1 can be orbitals, atoms, molecules, or fragments[54,67–84]. In addition, depending on the nature of the correlation problem or the available computational resources, any suitable algorithm can be chosen to predict the correlation energies, whether geared towards classical or quantum computing architectures. Some classical algorithms studied within the framework of the method of increments include the CC[71,76,79] and FCI approaches[54–56]. As for quantum algorithms, the phase estimation algorithm (PEA)[85,86] or the VQE[20] can be used.

B. Frozen natural orbitals

The method of increments is a technique that provides an efficient and accurate approach for computing electronic correlation energies. However, further reduction of the problem size will be required when we target applications on

near-term quantum computers. In the present study, we incorporate the FNO approach[57–61] into our framework to further reduce the problem size by truncating the virtual orbital space. In recent work, this approach has been applied to reduce the computational cost of quantum chemistry calculations in quantum computing[53].

FNOs are considered transformed and ranked virtual molecular orbitals. They are called "frozen" natural orbitals[87] as only the virtual–virtual block of the one-particle reduced density matrix is diagonalized. They can be obtained at any arbitrary level of an *ab initio* theory. In this work, we use the MBPT(1) wavefunction, which constitutes the first-order correction to the Hartree–Fock wavefunction. The one-particle virtual–virtual block of the MBPT(2) density matrix is diagonalized to obtain natural orbitals as eigenvectors and corresponding occupation numbers as eigenvalues. These eigenvalues can be used to truncate the virtual space, while the eigenvectors are employed to transform the virtual space. By choosing a certain threshold or population percentage criterion, a certain number of virtual orbitals can be kept, and the rest discarded.

The correlation energy is calculated only in the truncated virtual space, and then, the correction term $\Delta E^{\mathrm{MBPT(2)}} = E^{\mathrm{MO}}_{\mathrm{MBPT(2)}} - E^{\mathrm{FNO}}_{\mathrm{MBPT(2)}}$ is added to the correlation energy to recover the full correlation energy. The correction term $\Delta E^{\mathrm{MBPT(2)}}$ is the MBPT(2) correlation energy in the full molecular orbital space minus the MBPT(2) correlation energy in the truncated FNO space.

In the spin-orbital basis, the virtual–virtual (D_{ab}) block of the one-particle MBPT(2) density matrix is expressed as[59]

$$D^{(2)}_{\mathrm{ab}} = \frac{1}{2} \sum_{cij} \frac{\langle cb||ij\rangle \langle ij||ca\rangle}{\epsilon^{\mathrm{cb}}_{\mathrm{ij}} \epsilon^{\mathrm{ca}}_{\mathrm{ij}}} , \tag{6}$$

where the quantity ϵ^{ab}_{ij} in the denominator is defined as $\epsilon^{ab}_{ij} = f_{ii} + f_{jj} - f_{aa} - f_{bb}$, in which f is the Fock matrix. Note that $\langle cb||ij\rangle = \langle cb|ij\rangle - \langle cb|ji\rangle$ is an antisymmetric two-electron integral.

C. The Variational Quantum Eigensolver and the Unitary Coupled-Cluster (UCC) ansatz

We consider the VQE algorithm[20] as an example of the quantum solvers suitable for near-term applications on NISQ devices. The VQE algorithm was originally introduced, within the context of quantum chemistry, as a hybrid quantum–classical algorithm for solving the molecular electronic Schrödinger equation. According to the variational principle, for a (normalized) parametrization of the wavefunction $|\Psi(\vec{\theta})\rangle$, if one minimizes the expectation value of the Hamiltonian operator $\widehat{H}$

$$E = \langle \widehat{H} \rangle = \min_{\vec{\theta}} \langle \Psi(\vec{\theta})|\widehat{H}|\Psi(\vec{\theta})\rangle \geq E_{\mathrm{exact}} , \tag{7}$$

an upper bound to the exact ground state energy is obtained.

We wish to estimate values of the parameters $\{\theta_1, \theta_2, \ldots, \theta_p\}$ (i.e., the elements of the vector $\vec{\theta}$) that minimize the expectation value according to Eq. 7. The VQE algorithm requires a Hamiltonian operator in qubit form (i.e., written in terms of Pauli operators). Furthermore, a unitary parametric ansatz for the wavefunction, in the qubit basis, is required for the state preparation. Once the initial state has been prepared (i.e., an appropriate set of initial parameters has been used), an expectation value measurement is performed using quantum hardware or an appropriate simulation tool. Subsequently, the current value of the expectation value is fed to a classical optimizer in order to estimate a new set of variational parameters. This provides a new wavefunction, and the procedure is repeated until an optimized wavefunction and expectation value have been obtained.

The VQE algorithm constitutes a reduced circuit-depth hybrid quantum–classical methodology for solving the molecular electronic Schrödinger equation, as it minimizes the use of quantum hardware resources. In the second-quantization picture, the molecular electronic Hamiltonian takes the form

$$\widehat{H} = \sum_{p,q} h^p_q \hat{a}^\dagger_p a_q + \frac{1}{2} \sum_{p,q,r,s} h^{pq}_{rs} \hat{a}^\dagger_p \hat{a}^\dagger_q \hat{a}_s \hat{a}_r , \tag{8}$$

in which p, q, r, and s label general spin-orbitals, $a^\dagger_p$ and a_p are, respectively, creation and annihilation operators associated with orbital p. The one- and two-electron integrals, h^p_q and h^{pq}_{rs}, are

$$h^p_q = \langle p| \widehat{h} |q\rangle = \int \varphi^*_p(\mathbf{x}) \left(-\frac{1}{2}\nabla^2 - \sum_{\mu=1}^{\mathcal{N}} \frac{Z_\mu}{|\mathbf{r} - \mathbf{R}_\mu|} \right) \varphi_q(\mathbf{x}) \, \mathrm{d}\mathbf{x} \tag{9}$$

and

$$h_{rs}^{pq} = \langle pq|rs\rangle = \int \varphi_p^*(\mathbf{x}_1)\varphi_q^*(\mathbf{x}_2)\frac{1}{r_{12}}\varphi_r(\mathbf{x}_1)\varphi_s(\mathbf{x}_2)\,\mathrm{d}\mathbf{x}_1\mathrm{d}\mathbf{x}_2\,, \tag{10}$$

respectively, in which Z_μ and R_μ are the charge and position of nucleus μ, respectively, and $r_{12} = |\mathbf{r}_2 - \mathbf{r}_1|$ is the inter-electronic separation. The molecular Hamiltonian can be transformed into the qubit basis by using the Jordan–Wigner transformation[88] or another available transformation technique (e.g., Bravyi–Kitaev[89], Bravyi–Kitaev Superfast[90]):

$$\widehat{H} = \sum_p h_p^\alpha \sigma_p^\alpha + \sum_{pq} h_{pq}\sigma_p^\alpha \sigma_q^\beta + \sum_{pqr} h_{pqr}\sigma_p^\alpha \sigma_q^\beta \sigma_r^\gamma + \dots. \tag{11}$$

Here, p, q, r, ... label qubits, and σ_p^α, where $\alpha \in x, y, z$, is a Pauli matrix acting on qubit p.

While there are several strategies for deriving a parametric ansatz for the wavefunction (e.g., hardware efficient[9], QCC[30], and iQCC[31]), we consider the UCC ansatz in this work. The choice of ansatz is important for the convergence of the classical optimization and has a marked effect on the circuit depth. The latter issue is beyond the scope of the present study, but we plan to return to it in future work. Let us assume that the Hartree–Fock equations have been solved to obtain a zeroth-order, single-determinantal, mean-field wavefunction $|\Psi_0\rangle$ and the one- and two-electron integrals in the spin-orbital basis. As per convention, we use i, j, k, ... to label occupied spin-orbitals in the reference wavefunction, while a, b, c, ... are used to label unoccupied (virtual) orbitals. The UCC ansatz for the correlated wavefunction can then be written as

$$\Psi(\vec{\theta}) = e^{\widehat{T}-\widehat{T}^\dagger}|\Psi_0\rangle\,, \tag{12}$$

in which the cluster operator is defined as

$$\widehat{T} = \widehat{T}_1 + \widehat{T}_2 + \dots \tag{13}$$

$$= \sum_{i,a} \theta_i^a \hat{a}_a^\dagger \hat{a}_i + \frac{1}{2}\sum_{i,j,a,b} \theta_{ij}^{ab}\hat{a}_a^\dagger \hat{a}_b^\dagger \hat{a}_j \hat{a}_i + \dots \tag{14}$$

The UCC ansatz is usually truncated up to double excitations (i.e., including only $\widehat{T}_1$ and $\widehat{T}_2$ in Eq. 14), thus defining the UCC approach with single and double excitations (UCCSD). In analogy with the Hamiltonian in Eq. 11, the ansatz of Eq. 12 can be transformed into the qubit basis. Due to the non-commuting nature of the operators used in the UCCSD ansatz, the Suzuki–Trotter decomposition is used to decompose the exponential of the cluster operator as a product of unitary operators acting on the reference wavefunction (obtained from a classical Hartree–Fock calculation), and is subsequently transformed into a qubit representation. This Trotterized UCCSD ansatz is then used for the state preparation step of the VQE algorithm discussed above to find an approximate expectation value of the molecular electronic Hamiltonian, thus providing an estimate of the ground-state energy of a given molecule.

III. COMPUTATIONAL DETAILS

We carried out UCCSD and CCSD calculations using the incremental expansion approach and FNO-based virtual space truncation. The calculations were performed on the experimental molecular geometries of BeH_2, CH_4, NH_3, H_2O, and HF obtained from the NIST Computational Chemistry Comparison and Benchmark Database[91]. The cc-pVDZ basis set[62] was used for all of the calculations performed using these molecules.

In the incremental expansion approach, we considered the many-body expansion series including up to two-body terms for BeH_2, as the expansion including up to three-body terms becomes equivalent to solving the full problem (i.e., BeH_2 has three occupied orbitals). The expansion up to two-body terms for BeH_2 includes three one-body increments and three two-body increments—in total, six increments. For the rest of the molecules, CH_4, NH_3, H_2O, and HF, that have five occupied orbitals, we examined the expansions up to three and four bodies. The resulting total numbers of increments were 25 and 30, respectively, for the expansions up to three-body and four-body increments. For the virtual orbitals of each increment, we examined the effect of the size of the virtual space by adding one virtual orbital, which has a higher FNO occupancy, at a time, to the computational space of the increments.

For BeH_2, the electronic structure problems of the increments with a truncated virtual space up to seven virtual orbitals were solved by using VQE with the UCCSD ansatz, leading to, at most, an 18-qubit problem. As shown in following section, we found that the convergence behaviour of the solvers, UCCSD and CCSD, as a function of the number of virtual orbitals, closely resembled each other. Therefore, when the virtual space consisted of more than seven orbitals, the increments were solved using the conventional CCSD method. Furthermore, for the same reason,

only conventional CCSD calculations were performed for the molecules CH_4, NH_3, H_2O, and HF. The MBPT(2) FNO correction was added to the correlation energies obtained using a truncated virtual space, in order to account for the missing correlation energies. The resulting correlation energies for each increment were used to reconstruct the correlation energy of the entire molecule by following the expansion scheme described in the previous section. We refer to the present approach as MI(n)-FNO-UCCSD (or MI(n)-FNO-CCSD if the classical CCSD approach is used to obtain the correlation energy), where n indicates the expansion up to n-body increments. To obtain a qubit count estimation on an molecule relevant to industry, we considered a "constrained-geometry" metallocene olefin polymerization catalyst[92]. We used the experimental molecular geometry[92] and the cc-pVDZ and the cc-pVTZ basis sets[62].

The MI(n)-FNO-UCCSD and MI(n)-FNO-CCSD methods are part of *QEMIST*, the *Quantum-Enabled Molecular ab Initio Simulation Toolkit*[93], and the results of all the calculations described in the following section were performed using this software package. The molecular integrals were generated using PySCF[94]. The qubit representation of the molecular Hamiltonian was obtained using the Jordan–Wigner transformation[88] implemented in OpenFermion[95]. The VQE simulations using the UCCSD ansatz were performed using ProjectQ[96] and OpenFermion-ProjectQ[95]. The classical optimization steps of VQE were performed using the COBYLA algorithm[97] with a convergence tolerance of 10^{-5}. The MBPT(1) amplitudes were used as an initial guess of the parameters for the UCCSD trial wavefunction. The conventional CCSD energy of the full problem was also calculated by PySCF and used as a reference energy. In performing the conventional CCSD calculation, we used the tolerance of 10^{-7} hartrees.

IV.   RESULTS AND DISCUSSION

A.   Validation of the MI(n)-FNO approach

TABLE I. Total energy values (hartrees) and the difference from the conventional CCSD values using the MI(n)-CCSD approach. The differences are shown in parentheses. The calculated results for the many-body expansion truncated up to $n = 2$-, 3-, and 4-body increments are listed.

	CCSD	MI(2)-CCSD		MI(3)-CCSD		MI(4)-CCSD	
BeH_2	-15.835746	-15.835806	(-0.000060)	-15.835746	(0.000000)		
CH_4	-40.385951	-40.392778	(-0.006827)	-40.385350	(0.000601)	-40.385952	(-0.000001)
NH_3	-56.400579	-56.412272	(-0.011693)	-56.399440	(0.001140)	-56.400581	(-0.000002)
H_2O	-76.240099	-76.254995	(-0.014896)	-76.238622	(0.001478)	-76.240102	(-0.000003)
HF	-100.228154	-100.242731	(-0.014577)	-100.226824	(0.001331)	-100.228157	(-0.000003)

To validate the MI(n)-FNO approach, we first examined the accuracy of the energy calculations using the method of increments, with no virtual space truncation. The total energies of BeH_2, CH_4, NH_3, H_2O, and HF were calculated using the MI(2)-CCSD, MI(3)-CCSD, and MI(4)-CCSD methods, then comparing them with the conventional CCSD values. The total energies using the MI methods and the comparison of the energies with the CCSD energies are listed in Table I. We achieved chemical accuracy (0.0015 hartrees or 1.0 kcal/mol) with respect to the conventional CCSD value for the six-electron system BeH_2 using the MI(2) approach. The MI(3) value agrees with the parent CCSD value, because they are equivalent for this six-electron system. Hence, we found that MI(2) is sufficiently accurate for performing calculations on BeH_2. For the other four systems, each of which contain 10 electrons, we observed a relatively large error using the MI(2) expansion. The CH_4 molecule exhibited the smallest error, -0.006827 hartrees (4.28 kcal/mol), which is over four times larger than the target value of 1.0 kcal/mol for chemical accuracy. In contrast, with the MI(3) approach, we achieved chemical accuracy in the total energies for all molecules considered. The largest error was observed for the total energy of H_2O, which was 0.001478 hartrees (0.93 kcal/mol) larger than the CCSD value. The error became less than 5.0×10^{-6} hartrees when using MI(4) for these 10-electron systems. The accuracy of the MI(2) expansion was not sufficient for achieving chemical accuracy for the 10-electron systems considered in this work.

Therefore, as mentioned in Sec. III, the focus is on the MI(2) for BeH_2, and MI(3) and MI(4) for CH_4, NH_3, H_2O, and HF. The number of occupied orbitals in CCSD calculations was reduced by decomposing the original problem into subproblems (increments) using the MI expansion. For BeH_2, the MI(2) calculation included only two occupied orbitals, while three occupied orbitals were used in the CCSD calculation. For the other 10-electron systems, the MI(3) and MI(4) calculations included three and four occupied orbitals, respectively, while full CCSD calculation included five occupied orbitals. In this study, we used relatively small-sized molecules; thus, the reduction of occupied

orbitals was small. However, as we show later in this section, if we apply MI methods to larger-sized systems, we can achieve a large reduction in the number of occupied orbitals. Overall, we found that MI methods can recover accurate total energies while reducing computational cost.

TABLE II. Total energy values (hartrees) and the difference from the conventional CCSD values using MI(n)-FNO-CCSD approach. The differences are shown in parentheses. We employ an FNO population of 99% to determine the size of the virtual space.

	CCSD	MI-CCSD		MI-FNO-CCSD	
BeH_2 MI(2)	-15.835746	-15.835806	(-0.000060)	-15.836066	(-0.000320)
CH_4 MI(3)	-40.385951	-40.385350	(0.000601)	-40.385716	(0.000235)
CH_4 MI(4)	-40.385951	-40.385952	(-0.000001)	-40.386196	(-0.000245)
NH_3 MI(3)	-56.400579	-56.399440	(0.001140)	-56.399468	(0.001111)
NH_3 MI(4)	-56.400579	-56.400581	(-0.000002)	-56.400693	(-0.000114)
H_2O MI(3)	-76.240099	-76.238622	(0.001478)	-76.238514	(0.001585)
H_2O MI(4)	-76.240099	-76.240102	(-0.000003)	-76.239986	(0.000113)
HF MI(3)	-100.228154	-100.226824	(0.001331)	-100.226893	(0.001261)
HF MI(4)	-100.228154	-100.228157	(-0.000003)	-100.227998	(0.000156)

We next investigated the accuracy of molecular energy calculation using the MI approach, in conjunction with virtual space truncation based on the FNO approach (MI-FNO-CCSD). For the assessment of the accuracy, we chose the criterion of virtual orbital selection using a population percentage of 99%. This criterion has been used in previous FNO-CCSD calculations[57,58,60,61]. The total energies calculated using MI-FNO-CCSD, and their difference from the reference CCSD total energies are listed in Table II. Chemical accuracy was achieved for the total energies calculated with all the MI-FNO-CCSD approaches. The MI(3)-FNO-CCSD calculation on the H_2O molecule exhibited the largest error of 0.001478 hartrees (0.99 kcal/mol). The FNO approach reduces the number of virtual orbitals for each subproblem in the MI expansion. For BeH_2, using the MI(2) expansion, the FNO method with the threshold of 99% occupancy discarded 17, 5, and 7 virtual orbitals from the three one-body increments, and 5, 7, and 6 virtual orbitals from the three two-body increments, while the full problem of BeH_2 had 21 virtual orbitals. Therefore, the FNO method with a 99% threshold was able to discard at least five virtual orbitals. For the other 10-electron systems with the MI(3) expansion, the FNO approach discarded at least 7, 5, 3, and 2 virtual orbitals for the CH_4, NH_3, H_2O, and HF molecules, respectively. Again, we considered smaller systems in this work, so the reduction may not appear significant. However, we observed that the FNO virtual space truncation became more efficient as the virtual space became larger (for an example, see Sec. IV D). Previous studies[58,59,98] have shown that, even with significant truncation of the virtual space, based on the natural occupation numbers of the density matrix, employing FNOs leads to accurate calculation results for relative energies. Figure 2 shows the cumulative FNO occupancy percentage as a function of the number of virtual orbitals for the molecules we examined. The values on the horizontal axis represent the ratio of the number of virtual orbitals, calculated as "the number of virtual orbitals that are used in the calculation" divided by "the total number of virtual orbitals of the system". The dotted line shows the FNO occupancy of 99%. The plots were obtained by running FNO-CCSD calculations, not by using the MI-FNO-CCSD approach. As shown, the larger basis set reaches the 99% line sooner than the smaller basis sets. This means that the FNO truncation can discard more virtual orbitals as the virtual space becomes larger. Therefore, if we apply MI-FNO-CCSD to larger-sized systems or employ larger basis sets, we can achieve not only a considerable reduction in the number of occupied orbitals but also a significant reduction in the number of virtual orbitals. We found that the MI-FNO-CCSD method accurately recovers the total molecular energies, while reducing the computational cost, in comparison with their parent CCSD approaches.

B. The accuracy of MI(n)-FNO-UCCSD energies and qubits required

To investigate the accuracy of MI(n)-FNO-UCCSD energies and qubits required, we first performed MI-FNO-UCCSD calculations for BeH_2. The total energies calculated are listed in Table III. Quantum simulations of UCCSD on classical hardware require large computational resources compared to conventional CCSD; thus, we needed to reduce the computational cost to a greater degree. In general, due to the limitations of NISQ devices, we need to reduce the computational resources for a given wavefunction ansatz in our quantum simulations, compared to the scenario where we use classical hardware or have access to fault-tolerant quantum hardware. We examined how the computational cost could be reduced, by further reducing the size of the virtual space, without deteriorating the
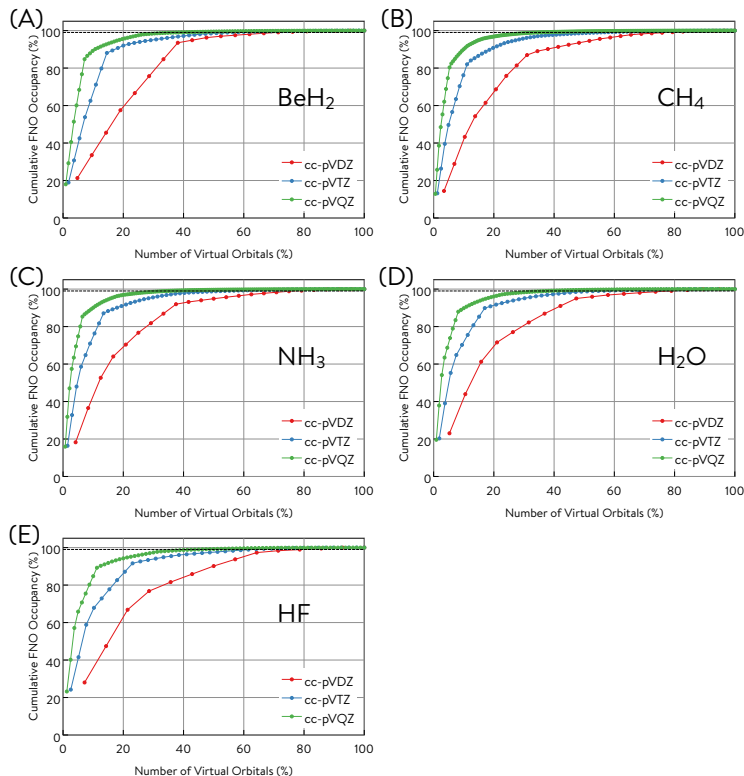
FIG. 2. Cumulative FNO occupancy as a function of the number of virtual orbitals for (A) BeH$_2$, (B) CH$_4$, (C) NH$_3$, (D) H$_2$O, and (E) HF.

TABLE III. Total energy values (hartrees) and the difference from the parent CCSD value (-15.835746 hartrees) using the MI(2)-FNO-UCCSD approach for BeH$_2$. The calculated results when using 1–7 virtual orbitals are listed.

Number of virtual orbitals	Total energy	Energy difference
1	-15.820990	0.014756
2	-15.826479	0.009267
3	-15.827018	0.008728
4	-15.827508	0.008238
5	-15.828969	0.006777
6	-15.832066	0.003680
7	-15.834886	0.000860

accuracy of the results as much as possible. Figure 3 shows how the total energy of BeH$_2$, using MI(2)-FNO-UCCSD, behaved as a function of the number of virtual orbitals. The plot presents the difference between the MI(2)-FNO-UCCSD and parent CCSD energies. The area filled in orange shows the region where deviations are within chemical accuracy. We see that the MI(2)-FNO-UCCSD values approached the reference CCSD energy as the number of virtual orbitals increases. When the number of virtual orbitals was seven, the difference from the reference energy became as small as 0.000860 hartrees or 0.54 kcal/mol, showing that chemical accuracy was reached. For this calculation, there were three one-body, 16-qubit increments (one occupied and seven virtual orbitals) and three two-body 18-qubit increments (two occupied and seven virtual orbitals). As the original problem required 48 qubits without PD, this was a large reduction in quantum resources; we believe that the present MI-FNO framework can help accelerate the practical application of near-term quantum hardware in quantum chemistry simulations. When the number of virtual orbitals was seven, we were able to discard 14 virtual orbitals. This roughly corresponds to the number of virtual orbitals discarded when the FNO 80% threshold was applied to all increments in order to truncate virtual orbitals.

To estimate the energy convergence behaviour as a function of the virtual space beyond 18 qubits, we first explored whether the MI(n)-FNO-CCSD approach could be used to extrapolate the MI(n)-FNO-UCCSD energies for the BeH$_2$ molecule. Varying the number of virtual orbitals from one to seven, we confirmed that the convergence behaviour of the MI(n)-FNO-UCCSD and MI(n)-FNO-CCSD approaches closely resembled each other. We then extended the MI(n)-FNO-CCSD calculations to the maximum number of virtual orbitals (21 in the present setup) to gain an understanding of the convergence of MI(2)-FNO-UCCSD energies. Based on this extrapolation, we found that MI(2)-FNO-UCCSD can provide chemically accurate results when the number of virtual orbitals is larger than seven.

Given that we observed that the MI-FNO-UCCSD approach can achieve chemical accuracy and that the energy convergence behaviours of MI-FNO-UCCSD and MI-FNO-CCSD closely resemble each other, we explored the energy convergence behaviour of the remaining molecules by using the MI-FNO-CCSD approach, as shown in Fig. 4 (A), (B), (C), and (D). As in the case of BeH$_2$, we found that MI(3)-FNO-CCSD approached the reference energy as the number of virtual orbitals was increased. The fewest qubits required to achieve chemical accuracy with respect to the parent CCSD values were 32, 32, 34, and 26 for CH$_4$, NH$_3$, H$_2$O, and HF, respectively, while the qubits necessary to perform a direct simulation of the full system were 68, 58, 48, and 38 for CH$_4$, NH$_3$, H$_2$O, and HF, respectively. The number of qubits and the number of subsystems required to achieve chemical accuracy by using the MI(n)-FNO-UCCSD approach are shown in Table IV.

TABLE IV. Number of qubits required to obtain chemical accuracy using the MI(n)-FNO-UCCSD approach. The number of qubits was estimated based on the energies obtained with the corresponding MI(n)-FNO-CCSD approach for CH$_4$, NH$_3$, H$_2$O, and HF. The numbers in parentheses indicate the number of increments the MI(n) approach generated.

	UCCSD	MI(2)-FNO-UCCSD	MI(3)-FNO-UCCSD	MI(4)-FNO-UCCSD
BeH$_2$	48	18 (6)		
CH$_4$	68		32 (25)	36 (30)
NH$_3$	58		32 (25)	32 (30)
H$_2$O	48		34 (25)	28 (30)
HF	38		26 (25)	24 (30)

For CH$_4$, NH$_3$, H$_2$O, and HF, the energy difference between MI(3)-FNO-CCSD and the reference CCSD energy, at the point where the number of virtual orbitals was equal to the maximum number of virtual orbitals, did not converge as well as in the case of BeH$_2$. For example, the MI(3)-FNO-CCSD energy of H$_2$O at the point where the number of virtual orbitals is equal to the full virtual space still has an error of 0.00148 hartrees from the reference. We speculate that this is due to the fact that the occupied orbitals were not spatially localized, and therefore the decomposition of the occupied space into a smaller occupied space based on the method of increments caused the residual error. The degree of the error may be mitigated by including higher-order body increments, so we examined the inclusion of four-body terms in the calculation (i.e., MI(4)-FNO-CCSD) as shown in Fig. 4 (A), (B), (C), and (D). In all cases considered, the inclusion of the four-body terms in the MI(4)-FNO-CCSD calculation largely improved the energy convergence towards the reference energy, and the energy at the point where the number of virtual orbitals was equal to the full virtual space differed from the reference energy by only around 5×10^{-5} hartrees or less. It is possible that the residual error, likely caused by the occupied orbitals not being spatially localized, can also be mitigated by using localized molecular orbitals. For example, we observed that using Foster–Boys localization[99] improved the energy convergence of MI(3)-FNO-CCSD towards the reference energy. We plan to discuss this improvement in more detail in future publications. The reason why we observed highly accurate results with the MI(4)-FNO-CCSD approach for these molecules may be because they are all 10-electron systems and the contribution from the core electrons is usually very small when the basis sets have no core-polarization functions, such as in the cc-pVDZ basis used here. We plan to investigate the convergence behaviour with respect to the order of bodies (e.g., three-body, four-body, fifth-body) in the many-body expansion in the MI-FNO approach by targeting larger molecular systems.

C. Quantum resource estimation for the MI(n)-FNO-UCCSD approach

Near-term quantum hardware will be limited not only in the number of qubits, but also in the number of gate operations. Therefore, it is important to understand the amount of quantum resources that will be needed to achieve the desired accuracy in electronic structure calculations, as discussed in the literature[52]. In this section, we discuss to what extent the MI(n)-FNO approach can reduce the quantum resources needed compared to full UCCSD simulation without PD. The number of one- and two-qubit gates we report are considered an upper bound of the gate counts,
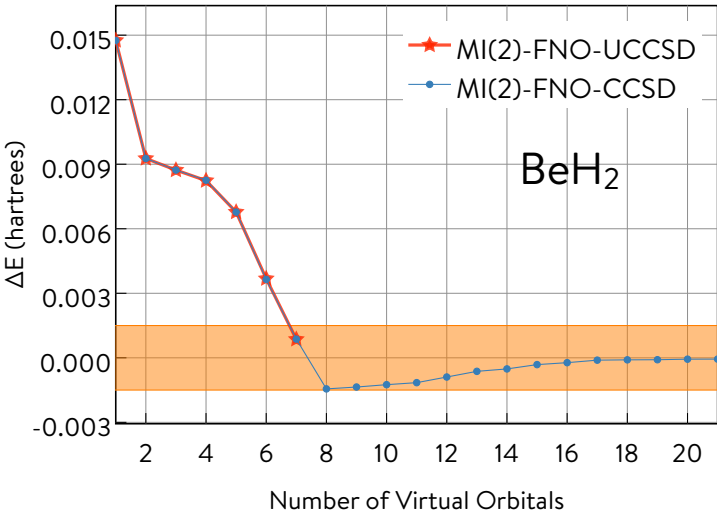
FIG. 3. Energy difference from the parent CCSD approach as a function of the number of virtual orbitals for the MI(2)-FNO-UCCSD and MI(2)-FNO-CCSD energies for BeH$_2$. The area filled in orange indicates where the results are within chemical accuracy from the reference energy.
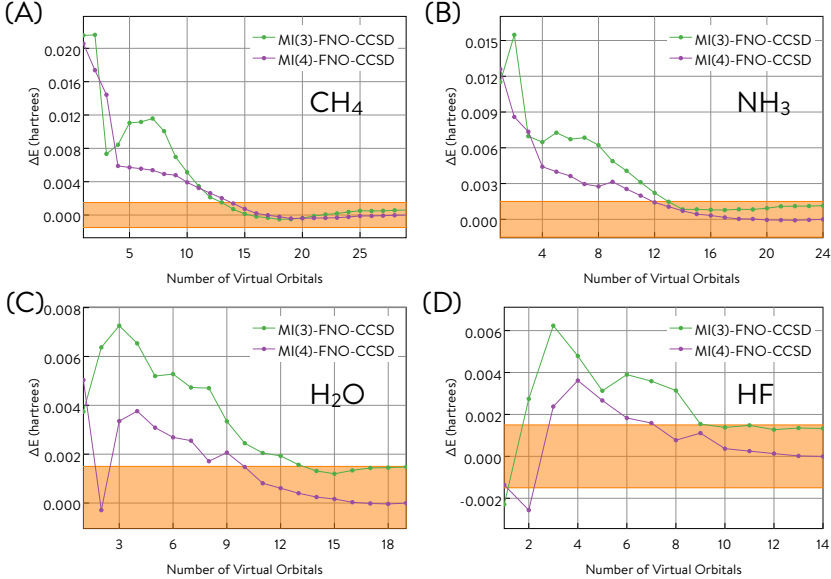

FIG. 4. Energy difference from the parent CCSD approach as a function of the number of virtual orbitals when using MI(3)-FNO-CCSD and MI(4)-FNO-CCSD for four molecules: (A)CH$_4$; (B) NH$_3$; (C) H$_2$O; and (D) HF. The area filled in orange indicates where the results are within chemical accuracy from the reference energy.

as the actual number of gate counts can vary depending on the level of circuit optimization. Using BeH$_2$ as an example, the MI(2)-FNO-UCCSD method achieved chemical accuracy when the number of virtual orbitals was seven (see Fig. 3), in which case we solved the electronic structure problem for three one-body 16-qubit increments and three two-body 18-qubits increments. Table V shows the amount of quantum resources required to solve the problem for the increments involved in this system. All of the three one-body increments required 16 qubits; however, as the complexity of the Hamiltonian was different in each case, the number of gate operations was also different. The same observation holds for two-body increments. In the worst-case analysis, the greatest number of one- and two-qubit gate counts needed to prepare the quantum state of the problem's increments were 4180 and 6944 gates, respectively. We consider these numbers to represent the quantum resources required to achieve chemically accurate energies in the framework of the MI(2)-FNO-UCCSD approach.

Table VI gives a summary of the quantum resources required to achieve chemically accurate energies for all the

TABLE V. Quantum resources for each increment generated by the MI-FNO approach for BeH_2. The percentages in parentheses indicate the amount of reduction that the MI(2)-FNO approach achieves.

	# of qubits	# of one-qubit gates	# of two-qubit gates
one-body (1)	16 (66.7%)	794 (98.9%)	848 (99.7%)
one-body (2)	16 (66.7%)	650 (99.1%)	464 (99.8%)
one-body (3)	16 (66.7%)	794 (98.9%)	1104 (99.6%)
two-body (1,2)	18 (62.5%)	2740 (96.3%)	2304 (99.2%)
two-body (1,3)	18 (62.5%)	4180 (94.3%)	6816 (97.7%)
two-body (2,3)	18 (62.5%)	3892 (94.7%)	6944 (97.7%)
Full system	48	73,230	302,160

molecules have examined. Also shown is the degree of reduction the MI(n)-FNO-UCCSD approach was able to provide. We found that our MI(n)-FNO-UCCSD approach considerably reduced the number of gate operations: by 74% to 98% from those required for full UCCSD simulation without PD. The resulting number of gate operations remains very large for near-term quantum hardware; however, our MI(n)-FNO approach is general, and can be combined with any other ansatzes that may provide shallower circuits than UCCSD, such as the "hardware-efficient" ansatz[26] and QCC methods[30,31].

TABLE VI. Quantum resources required to obtain chemically accurate energies. The number before the slash represents the quantum resources needed when using the MI(n)-FNO approach, and the number after the slash represents the quantum resources required for full UCCSD simulation without PD. The percentages given in parentheses represent the extent of reduction that the MI(n)-FNO approach achieved.

	# of qubits	# of one-qubit gates	# of two-qubit gates
BeH_2	18/48 (63%)	4180/73,230 (94%)	6944/302,160 (98%)
CH_4	32/68 (53%)	143,214/1,726,498 (92%)	384,592/9,482,448 (96%)
NH_3	32/58 (45%)	103,830/731,602 (86%)	275,520/3,373,264 (92%)
H_2O	34/48 (29%)	62,934/241,138 (74%)	182,592/929,648 (80%)
HF	26/38 (32%)	36,870/205,498 (82%)	83,328/660,032 (87%)

D. Qubit count estimation for an industrial catalyst molecule

In this section, we provide qubit count estimations for the "constrained-geometry" metallocene olefin polymerization catalyst ("CGC")[92] (see Fig. 6), as an early indication of the efficacy of the MI(n)-FNO approach for molecular systems relevant to industry. The experimental molecular geometry of CGC[92] and the cc-pVDZ and the cc-pVTZ basis sets[62] were used. In Table VII, we summarize the qubit count estimations when only the FNO virtual space truncation was applied and when the MI(3)-FNO approach was applied. In order to estimate the number of qubits for the FNO virtual space truncation, we added the number of FNO virtual orbitals (N_v) after truncation to the number of occupied orbitals N_{occ} in the system. The number of virtual orbitals N_v in the FNO approach was determined based on a given percentage of FNO occupancy for the full molecular system. So, the total qubit count was obtained using $2(N_v + N_{occ})$. In the qubit count estimation for the MI(3)-FNO approach, the maximum number of occupied orbitals was three, corresponding to the three-body increments in the MI(3) expansion. Hence, the total qubit count in Table VII was obtained using $2(N_v + 3)$. This is a rough estimate of the necessary number of qubits needed for the MI(3)-FNO approach, and a more accurate assessment is needed. The number of qubits needed when employing the MI(3) approach on its own was 784. When employing the largest value of the FNO percentage (99%) to truncate the virtual space, the MI(3)-FNO approach reduced the qubit requirements by almost half. Considering that the MI-FNO approach with 99% FNO occupancy produced very accurate results, as shown in Sec. IV A (see Table II), we speculate that we can obtain similar results for larger molecules. The number of qubits drastically decreased as we truncated the virtual space to a greater degree. Comparison of the qubit count between the FNO and MI(3)-FNO approaches showed that the MI(3)-FNO approach had a smaller qubit requirement than the FNO approach, regardless of the FNO occupancy threshold. Also, we observed that the advantage of the MI(3)-FNO approach over the FNO approach became clearer as the FNO occupancy became smaller, resulting in the number of virtual orbitals in the computational
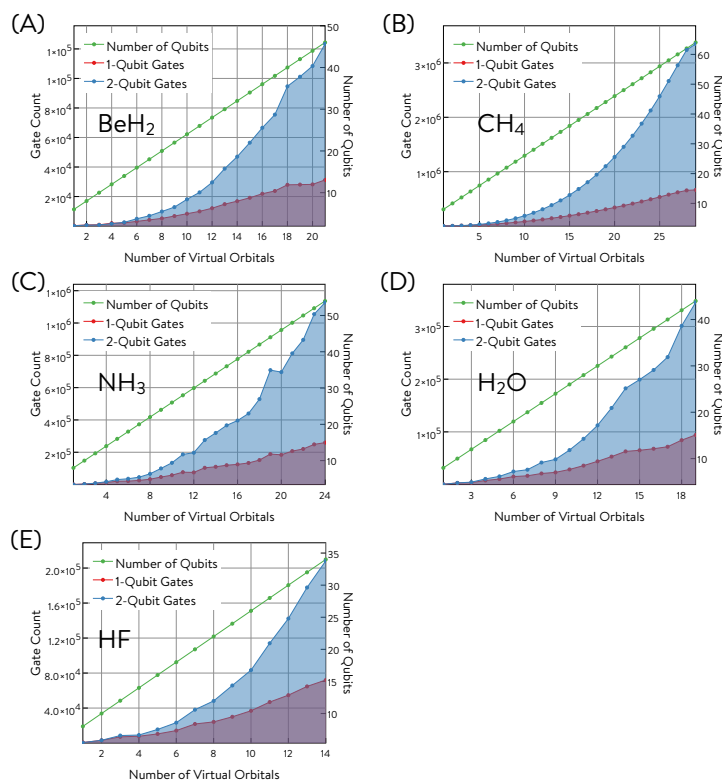
FIG. 5. Quantum resources required to prepare the quantum state of the subsystem as a function of the number of virtual orbitals. The MI(n)-FNO approach produces many increments, and the quantum resources that are required for an increment vary depending on the increment. The largest numbers of qubit, one- and two-qubit gate counts are plotted.

space becoming small and the number of occupied orbitals becoming dominant in the computational space. Therefore, we believe that the MI-FNO approach can be beneficial when targeting larger molecular systems in which there are many occupied orbitals. The number of increments in the MI-FNO approach becomes large as the number of occupied orbitals in the system becomes large (the CGC molecule has about 117,569 increments in the three-body expansion). However, the electronic structure problem can be solved independently for each increment; thus, these problems can be solved in parallel. Furthermore, we can discard small increments by using either distance- or energy-based screening, or a domain-based approach[71,79] can help us reduce the number of increments while maintaining the accuracy level of the calculation. It would be interesting to explore what the minimal quantum resource requirements would be for achieving chemical accuracy in the total energies in the case of these larger molecular systems after implementing a highly parallel framework.
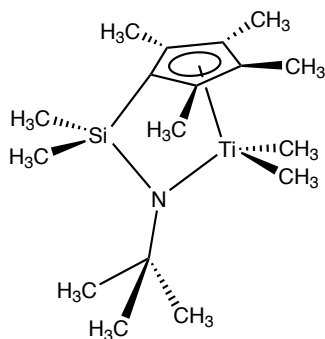

FIG. 6. Molecular structure of CGC

TABLE VII. Qubit count estimation for the CGC molecule. The molecule has 89 occupied and 389 virtual orbitals.

FNO occupancy	cc-pVDZ		cc-pVTZ	
	FNO	MI(3)-FNO	FNO	MI(3)-FNO
99%	768	596	1298	1126
90%	452	280	556	384
80%	376	204	408	236
70%	324	152	348	176
60%	286	114	304	132
50%	256	84	268	96
40%	232	60	240	68
30%	212	40	216	44
20%	196	24	198	26
10%	186	14	186	14
Full system	956		2208	

V. CONCLUSION

Quantum computing is a new computing paradigm that has the potential to accelerate the materials innovation process. In the era of noisy, intermediate-scale quantum (NISQ) devices, reducing the problem size of molecular systems is essential in helping to advance the application of quantum computing in materials science and life science. At the same time, it could provide opportunities for the further characterization of the usefulness of NISQ devices for quantum chemistry simulations by allowing us to conduct hardware experiments based on smaller, yet more realistic, chemistry problems.

In this paper, we have described a novel framework for the systematic reduction of both the occupied and virtual spaces in quantum chemistry simulations on near-term quantum devices. This framework employs the method of increments (MI) in conjunction with frozen natural orbitals (FNO). This method, referred to as the MI-FNO approach, distributes the occupied orbitals among subproblems (or increments) based on the many-body expansion of the correlation energy in terms of occupied orbital space, and truncates the virtual orbital space based on FNOs, which are obtained using the one-particle density matrix from second-order, many-body perturbation theory.

The framework of the MI-FNO approach is not tied to any particular method of predicting the correlation energy of the increments, so one can employ any algorithm, including conventional quantum chemistry methods, such as FCI and CC, and quantum algorithms, such as the phase estimation algorithm and the variational quantum eigensolver (VQE). As a demonstration of the applicability of the MI-FNO approach to the quantum computing framework, we used VQE in combination with unitary coupled-cluster (UCC) ansatz, the parametric ansatz employed in our study.

We refer to this combined framework as the MI(n)-FNO-UCCSD approach (or the MI(n)-FNO-CCSD approach if the classical CCSD method is used to obtain the correlation energy), where n indicates the expansion up to n-body increments. We examined its accuracy and feasibility by studying small molecules, namely, BeH_2, CH_4, NH_3, H_2O, and HF, in a cc-pVDZ basis set. We observed that the MI-FNO approach can achieve chemical accuracy by significantly reducing both the number of qubits and the number of gate operations, which suggests that it can be used to build a scalable quantum chemistry simulation platform on quantum hardware. Furthermore, as an early demonstration of the efficacy of our approach for larger molecules, we presented a qubit count estimation on an industrially relevant molecule, "constrained-geometry catalyst" (CGC), for olefin polymerization, as a representative catalyst. We found that, even by employing a modest truncation of the virtual space using 99% of the FNO occupancy, the MI-FNO approach reduced the qubit requirements by almost a factor of one half. We plan to perform MI-FNO calculations for large molecules, including CGC, and identify the quantum resources required to achieve chemical accuracy in the energy calculations. These calculations would allow us to build a comprehensive table to determine the relationship between the accuracy of the results, the orders of the many-body expansion, and the FNO occupancy. Such a table would help establish a framework for identifying both the optimal order of many-body expansion and the optimal FNO occupancy threshold in an a priori fashion, which would make the MI-FNO approach more practical.

In addition to the capability of reducing the computational requirements of the electronic structure calculation while maintaining the level of accuracy, the MI-FNO approach has another advantage: calculations of the electronic structure problem for each increment can be performed in a highly parallel manner. In practice, this advantage provides us with several computational options, making it possible to adapt the demands of a calculation to the evolving performance envelope of quantum hardware devices by employing both classical and quantum hardware in a flexible manner.

Our MI-FNO approach is one of the core methodologies included in *QEMIST*, the *Quantum-Enabled Molecular ab Initio Simulation Toolkit*[93], our new software package designed to run on both quantum and classical hardware back ends. It can assist in scaling up the size of molecular systems that can be simulated in quantum chemistry applications through various types of problem decomposition techniques, aiding computational chemistry studies for large-scale industrial applications.

ACKNOWLEDGEMENTS

REFERENCES

[1] M. Head-Gordon and E. Artacho, Physics Today **61**, 58 (2008).
[2] Y. Manin, *Vychislimoe i Nevychislimoe (Computable and Noncomputable)* (Sovetskoye Radio, Moscow, 1980) pp. 13–15.
[3] R. Feynman, International Journal of Theoretical Physics **21**, 467 (1982).
[4] S. Lloyd, Science **273**, 1073 (1996).
[5] A. Aspuru-Guzik, A. D. Dutoi, P. J. Love, and M. Head-Gordon, Science **309**, 1704 (2005).
[6] A. Peruzzo, J. McClean, P. Shadbolt, M.-H. Yung, X.-Q. Zhou, P. J. Love, A. Aspuru-Guzik, and J. L. O'Brien, Nature Communications **5** (2014).
[7] C. Hempel, C. Maier, J. Romero, J. McClean, T. Monz, H. Shen, P. Jurcevic, B. P. Lanyon, P. Love, R. Babbush, A. Aspuru-Guzik, R. Blatt, and C. F. Roos, Phys. Rev. X **8**, 031022 (2018).
[8] P. J. J. O'Malley, R. Babbush, I. D. Kivlichan, J. Romero, J. R. McClean, R. Barends, J. Kelly, P. Roushan, A. Tranter, N. Ding, B. Campbell, Y. Chen, Z. Chen, B. Chiaro, A. Dunsworth, A. G. Fowler, E. Jeffrey, E. Lucero, A. Megrant, J. Y. Mutus, M. Neeley, C. Neill, C. Quintana, D. Sank, A. Vainsencher, J. Wenner, T. C. White, P. V. Coveney, P. J. Love, H. Neven, A. Aspuru-Guzik, and J. M. Martinis, Phys. Rev. X **6**, 031007 (2016).
[9] A. Kandala, A. Mezzacapo, K. Temme, M. Takita, M. Brink, J. M. Chow, and J. M. Gambetta, Nature **549**, 242 (2017).
[10] Y. Nam, J.-S. Chen, N. C. Pisenti, K. Wright, C. Delaney, D. Maslov, K. R. Brown, S. Allen, J. M. Amini, J. Apisdorf, K. M. Beck, A. Blinov, V. Chaplin, M. Chmielewski, C. Collins, S. Debnath, A. M. Ducore, K. M. Hudek, M. Keesan, S. M. Kreikemeier, J. Mizrahi, P. Solomon, M. Williams, J. D. Wong-Campos, C. Monroe, and J. Kim, arXiv.org , arXiv:1902.10171v2 [quant (2019).
[11] https://www.ibm.com/quantum-computing/.
[12] https://ai.google/research/teams/applied-science/quantum/.
[13] https://newsroom.intel.com/press-kits/quantum-computing/.
[14] https://www.rigetti.com/.
[15] https://quantumcircuits.com.
[16] https://ionq.com/.
[17] https://www.honeywell.com/en-us/company/quantum.
[18] F. Arute, K. Arya, R. Babbush, D. Bacon, J. C. Bardin, R. Barends, R. Biswas, S. Boixo, F. G. S. L. Brandao, D. A. Buell, B. Burkett, Y. Chen, Z. Chen, B. Chiaro, R. Collins, W. Courtney, A. Dunsworth, E. Farhi, B. Foxen, A. Fowler, C. Gidney, M. Giustina, R. Graff, K. Guerin, S. Habegger, M. P. Harrigan, M. J. Hartmann, A. Ho, M. Hoffmann, T. Huang, T. S. Humble, S. V. Isakov, E. Jeffrey, Z. Jiang, D. Kafri, K. Kechedzhi, J. Kelly, P. V. Klimov, S. Knysh, A. Korotkov, F. Kostritsa, D. Landhuis, M. Lindmark, E. Lucero, D. Lyakh, S. Mandrà, J. R. McClean, M. McEwen, A. Megrant, X. Mi, K. Michielsen, M. Mohseni, J. Mutus, O. Naaman, M. Neeley, C. Neill, M. Y. Niu, E. Ostby, A. Petukhov, J. C. Platt, C. Quintana, E. G. Rieffel, P. Roushan, N. C. Rubin, D. Sank, K. J. Satzinger, V. Smelyanskiy, K. J. Sung, M. D. Trevithick, A. Vainsencher, B. Villalonga, T. White, Z. J. Yao, P. Yeh, A. Zalcman, H. Neven, and J. M. Martinis, Nature **574**, 505 (2019).
[19] J. Preskill, Quantum **2**, 79 (2018).
[20] A. Peruzzo, J. McClean, P. Shadbolt, M.-H. Yung, X.-Q. Zhou, P. J. Love, A. Aspuru-Guzik, and J. L. O'Brien, Nat. Commun. **5**, 4213 (2014).
[21] M. Ganzhorn, D. J. Egger, P. K. Barkoutsos, P. Ollitrault, G. Salis, N. Moll, A. Fuhrer, P. Mueller, S. Woerner, I. Tavernelli, and S. Filipp, arXiv.org , arXiv:1809.05057 [quant (2018).
[22] K. M. Nakanishi, K. Mitarai, and K. Fujii, arXiv.org , arXiv:1810.09434 [quant (2018).
[23] S. Matsuura, T. Yamazaki, V. Senicourt, L. Huntington, and A. Zaribafiyan, arXiv.org , arXiv:1810.11511.
[24] P. J. J. O'Malley, R. Babbush, I. D. Kivlichan, J. Romero, J. R. McClean, R. Barends, J. Kelly, P. Roushan, A. Tranter, N. Ding, B. Campbell, Y. Chen, Z. Chen, B. Chiaro, A. Dunsworth, A. G. Fowler, E. Jeffrey, E. Lucero, A. Megrant, J. Y. Mutus, M. Neeley,

C. Neill, C. Quintana, D. Sank, A. Vainsencher, J. Wenner, T. C. White, P. V. Coveney, P. J. Love, H. Neven, A. Aspuru-Guzik, and J. M. Martinis, Physical Review X **6**, 031007 (2016).

[25] J. Romero, R. Babbush, J. R. McClean, C. Hempel, P. Love, and A. Aspuru-Guzik, arXiv.org , 1701.02691 (2017).

[26] A. Kandala, A. Mezzacapo, K. Temme, M. Takita, M. Brink, J. M. Chow, and J. M. Gambetta, Nature **549**, 242 EP (2017).

[27] R. Babbush, N. Wiebe, J. McClean, J. McClain, H. Neven, and G. K.-L. Chan, arXiv.org , arXiv:1706.00023 (2017).

[28] I. D. Kivlichan, J. McClean, N. Wiebe, C. Gidney, A. Aspuru-Guzik, G. K.-L. Chan, and R. Babbush, arXiv.org , arXiv:1711.04789 (2017).

[29] H. R. Grimsley, S. E. Economou, E. Barnes, and N. J. Mayhall, arXiv.org , arXiv:1812.11173 [quant (2018).

[30] I. G. Ryabinkin, T.-C. Yen, S. N. Genin, and A. F. Izmaylov, Journal of Chemical Theory and Computation **14**, 6317 (2018).

[31] I. G. Ryabinkin and S. N. Genin, arXiv.org , arXiv:1906.11192 (2019).

[32] B. Bauer, D. Wecker, A. J. Millis, M. B. Hastings, and M. Troyer, arXiv.org , arXiv:1510.03859 (2016).

[33] M. Reiher, N. Wiebe, K. M. Svore, D. Wecker, and M. Troyer, Proceedings of the National Academy of Sciences **114**, 7555 (2017).

[34] N. C. Rubin, arXiv.org , arXiv:1610.06910 (2016).

[35] C. Hempel, C. Maier, J. Romero, J. McClean, T. Monz, H. Shen, P. Jurcevic, B. Lanyon, P. Love, R. Babbush, A. Aspuru-Guzik, R. Blatt, and C. Roos, arXiv.org , arXiv:1803.10238 (2018).

[36] T. Yamazaki, S. Matsuura, A. Narimani, A. Saidmuradov, and A. Zaribafiyan, arXiv.org , arXiv:1806.01305 (2018).

[37] Q. Gao, H. Nakamura, T. P. Gujarati, G. O. Jones, J. E. Rice, S. P. Wood, M. Pistoia, J. M. Garcia, and N. Yamamoto, arXiv.org , arXiv:1906.10675 (2019).

[38] O. Sinanoğlu, "Many-electron theory of atoms, molecules and their interactions," in *Advances in Chemical Physics* (John Wiley & Sons, Ltd, 2007) pp. 315–412, https://onlinelibrary.wiley.com/doi/pdf/10.1002/9780470143520.ch7.

[39] R. K. Nesbet, "Electronic correlation in atoms and molecules," in *Advances in Chemical Physics* (John Wiley & Sons, Ltd, 2007) pp. 321–363, https://onlinelibrary.wiley.com/doi/pdf/10.1002/9780470143551.ch4.

[40] R. Ahlrichs and W. Kutzelnigg, The Journal of Chemical Physics **48**, 1819 (1968), https://doi.org/10.1063/1.1668917.

[41] M. A. Collins and R. P. A. Bettens, *Chemical Reviews*, Chemical Reviews **115**, 5607 (2015).

[42] K. Raghavachari and A. Saha, *Chemical Reviews*, Chemical Reviews **115**, 5643 (2015).

[43] Q. Sun and G. K.-L. Chan, Accounts of Chemical Research **49**, 2705 (2016).

[44] G. A. N. J., "Frontiers of quantum chemistry," (Springer, Singapore, 2018) Chap. Embedding Methods in Quantum Chemistry.

[45] F. Neese, F. Wennmohs, and A. Hansen, The Journal of Chemical Physics **130**, 114108 (2009), https://doi.org/10.1063/1.3086717.

[46] F. Neese, A. Hansen, and D. G. Liakos, The Journal of Chemical Physics **131**, 064103 (2009), https://aip.scitation.org/doi/pdf/10.1063/1.3173827.

[47] C. Riplinger and F. Neese, The Journal of Chemical Physics **138**, 034106 (2013), https://doi.org/10.1063/1.4773581.

[48] C. Riplinger, B. Sandhoefer, A. Hansen, and F. Neese, The Journal of Chemical Physics **139**, 134101 (2013), https://doi.org/10.1063/1.4821834.

[49] C. Riplinger, P. Pinski, U. Becker, E. F. Valeev, and F. Neese, The Journal of Chemical Physics **144**, 024109 (2016), https://doi.org/10.1063/1.4939030.

[50] G. Schmitz and C. Hättig, The Journal of Chemical Physics **145**, 234107 (2016), https://doi.org/10.1063/1.4972001.

[51] M. Schwilk, Q. Ma, C. Köppl, and H.-J. Werner, *Journal of Chemical Theory and Computation*, Journal of Chemical Theory and Computation **13**, 3650 (2017).

[52] M. Kühn, S. Zanker, P. Deglmann, M. Marthaler, and H. Weiß, arXiv.org , arXiv:1812.06814 (2018).

[53] Y. Mochizuki, K. Okuwaki, T. Kato, and Y. Minato, (2019), 10.26434/chemrxiv.9863810.v1.

[54] P. M. Zimmerman, The Journal of Chemical Physics **146**, 104102 (2017).

[55] P. M. Zimmerman, The Journal of Physical Chemistry A **121**, 4712 (2017).

[56] P. M. Zimmerman, The Journal of Chemical Physics **146**, 224104 (2017).

[57] A. G. Taube and R. J. Bartlett, The Journal of Chemical Physics **128**, 044110 (2008), https://doi.org/10.1063/1.2830236.

[58] A. G. Taube and R. J. Bartlett, Collection of Czechoslovak Chemical Communications **70**, 837 (2005).

[59] A. G. Taube and R. J. Bartlett, The Journal of Chemical Physics **128**, 164101 (2008).

[60] C. Sosa, J. Geertsen, G. W. Trucks, R. J. Bartlett, and J. A. Franz, Chemical Physics Letters **159**, 148 (1989).

[61] H. J. A. Jensen, P. Jo/rgensen, H. gren, and J. Olsen, The Journal of Chemical Physics **88**, 3834 (1988), https://doi.org/10.1063/1.453884.

[62] T. H. Dunning, *The Journal of Chemical Physics*, The Journal of Chemical Physics **90**, 1007 (1989).

[63] R. K. Nesbet, Phys. Rev. **155**, 51 (1967).

[64] R. K. Nesbet, Phys. Rev. **155**, 56 (1967).

[65] R. K. Nesbet, Phys. Rev. **175**, 2 (1968).

[66] H. A. Bethe and J. Goldstone, Proc. R. Soc. A **238**, 551 (1957).

[67] H. Stoll, Chemical Physics Letters **191**, 548 (1992).

[68] M. Mödll, M. Dolg, P. Fulde, and H. Stoll, Journal of Chemical Physics **106**, 1836 (1997).

[69] V. Bezugly and U. Birkenheuer, Chemical Physics Letters **399**, 57 (2004).

[70] H. Stoll, B. Paulus, and P. Fulde, The Journal of Chemical Physics **123**, 144108 (2005).

[71] J. Friedrich, M. Hanrath, and M. Dolg, The Journal of Chemical Physics **126**, 154110 (2007).

[72] E. E. Dahlke and D. G. Truhlar, Journal of Chemical Theory and Compuation **3**, 46 (2007).

[73] L. Bytautas and K. Ruedenberg, Journal of Physical Chemistry A **114**, 8601 (2010).

[74] M. S. Gordon, D. G. Fedorov, S. R. Pruitt, and L. V. Slipchenko, Chemical Reviews **112**, 632 (2012).

[75] C. Müller and B. Paulus, Physical Chemistry Chemical Physics **14**, 7605 (2012).

[76] J. Zhang and M. Dolg, Journal of Chemical Theory and Computation **9**, 2992 (2013).

[77] R. M. Richard, K. U. Lao, and J. M. Herbert, The Journal of Chemical Physics **141**, 014108 (2014).

[78] E. Voloshina and B. Paulus, Journal of Chemical Theory and Computation **10**, 1698 (2014).

[79] T. Anacker, D. P. Tew, and J. Friedrich, *Journal of Chemical Theory and Computation*, Journal of Chemical Theory and Computation **12**, 65 (2016).

[80] K. U. Lao, K.-Y. Liu, R. M. Richard, and J. M. Herbert, The Journal of Chemical Physics **144**, 164105 (2016).

[81] J. J. Eriksen, F. Lipparini, and G. J., Journal of Physical Chemistry Letters **8**, 4633 (2017).

[82] J. S. Boschen, D. Theis, K. Ruedenberg, and T. L. Windus, Journal of Physical Chemistry A **121**, 836 (2017).

[83] E. Fertitta, D. Koch, B. Paulus, G. Barcza, and Ö. Legeza, Molecular Physics **116**, 1471 (2018).

[84] P. M. Zimmerman and A. E. Rask, **150**, 244117 (2019).

[85] D. S. Abrams and S. Lloyd, Physical Review Letters **79**, 2586 (1997).

[86] A. Aspuru-Guzik, A. D. Dutoi, P. J. Love, and M. Head-Gordon, Science **309**, 1704 (2005).

[87] P.-O. Löwdin, Phys. Rev. **97**, 1474 (1955).

[88] P. Jordan and E. Wigner, Zeitschrift für Physik **47**, 631 (1928).

[89] S. B. Bravyi and A. Y. Kitaev, Annals of Physics **298**, 210 (2002).

[90] K. Setia and J. D. Whitfield, The Journal of Chemical Physics **148**, 164104 (2018).

[91] "NIST CCCDB: National Institute of Standards and Technology Computational Chemistry Comparison and Benchmark DataBase," https://cccbdb.nist.gov.

[92] D. J. Arriola, M. Bokota, R. E. Campbell, J. Klosin, R. E. LaPointe, O. D. Redwine, R. B. Shankar, F. J. Timmers, and K. A. Abboud, Journal of the American Chemical Society **129**, 7065 (2007).

[93] "QEMIST: Quantum-Enabled Molecular ab-Initio Simulation Toolkit," https://1qbit.com/qemist/.

[94] Q. Sun, T. C. Berkelbach, N. S. Blunt, G. H. Booth, S. Guo, Z. Li, J. Liu, J. D. McClain, E. R. Sayfutyarova, S. Sharma, S. Wouters, and G. K.-L. Chan, Wiley Interdisciplinary Reviews: Computational Molecular Science **8**, e1340 (2018).

[95] J. R. McClean, I. D. Kivlichan, D. S. Steiger, K. J. Sung, Y. Cao, C. Dai, E. S. Fried, C. Gidney, T. Häner, V. Havlíček, C. Huang, Z. Jiang, M. Neeley, J. Romero, N. Rubin, N. P. D. Sawaya, K. Setia, S. Sim, W. Sun, F. Zhang, and R. Babbush, arXiv.org , arXiv:1710.07629 [quant (2017).

[96] D. S. Steiger, T. Häner, and M. Troyer, Quantum **2**, 49 (2018).

[97] M. J. D. Powell, "Advances in optimization and numerical analysis," (Kluwer Academic, Dordrecht, 1994) Chap. A direct search optimization method that models the objective and constraint functions by linear interpolation, pp. 51–67.

[98] A. Landau, K. Khistyaev, S. Dolgikh, and A. I. Krylov, The Journal of Chemical Physics **132**, 014109 (2010).

[99] J. M. Foster and S. F. Boys, Reviews of Modern Physics **32**, 300 (1960).